PhaseFi: Phase Fingerprinting for Indoor Localization with a Deep Learning Approach

Xuyu Wang, Lingjun Gao, and Shiwen Mao
Department of Electrical and Computer Engineering, Auburn University, Auburn, AL 36849-5201
Email: {xzw0029, lzg0014}@auburn.edu, smao@ieee.org

***Abstract*—With the increasing demand of location-based services, indoor localization based on fingerprinting has become an increasingly important technique due to its high accuracy and low hardware requirement. In this paper, we propose PhaseFi, a fingerprinting system for indoor localization with calibrated channel state information (CSI) phase information. In PhaseFi, the raw phase information is first extracted from the multiple antennas and multiple subcarriers of the IEEE 802.11n network interface card (NIC) by accessing the modified driver. Then a linear transform is used to extract the calibrated phase information, which is proven to have a bounded variance. For the offline stage, we design a deep network with three hidden layers to train the calibrated phase data, and employ weights to represent fingerprints. A greedy learning algorithm is incorporated to train the weights layer-by-layer to reduce computational complexity, where a sub-network between two continuous layers forms a Restricted Boltzmann Machine (RBM). In the online stage, we use a probabilistic method based on the radial basis function (RBF) for online location estimation. The proposed PhaseFi scheme is implemented and validated with intensive experiments in two representation indoor environments. It outperforms other three benchmark schemes based on CSI or RSS in both scenarios.**

I. Introduction

In this paper, we investigate the problem of accurate fingerprinting based indoor localization. As one of the popular schemes for indoor localization, a fingerprinting-based approach first builds a database with thorough measurements of the field and then infers the real-time location by comparing the new measurements with database data [1]–[6].

Many existing indoor fingerprinting systems utilize WiFi received signal strength (RSS) values as fingerprints due to the simplicity and low hardware requirements. For example, Radar is the first fingerprinting system based on RSS with a deterministic method for location estimation [3]. Later, Horus utilizes a probabilistic method for indoor localization with RSS values [6], which achieves better localization accuracy than Radar. Such RSS based methods have two main disadvantages. First, RSS values are highly random and its correlation with propagation distance is loose due to shadowing fading and multipath effects. Second, RSS values are coarse information obtained by averaging the amplitudes of all incoming signals, and the channel information from different subcarriers is not used. Thus, localization based on RSS values may lead to poor localization performance.

By modifying the device driver, we can now obtain channel state information (CSI) from some advanced WiFi network interface cards (NIC), such as the Intel WiFi Link 5300 NIC [7], [8]. CSI values provide subcarrier-level channel measurements, which can be very helpful for indoor fingerprinting. For example, FIFS [9] utilizes the weighted average CSI values over multiple antennas to improve the performance of RSS-based method for indoor fingerprinting. Another work, DeepFi [10] learns a large amount of CSI data from three antennas for indoor localization based on a deep network. However, these schemes only consider the amplitude of CSI, and the CSI phase information is ignored, which is largely due to the randomness and unavailability of the raw phase information. To the best of our knowledge, CSI-MIMO [11] incorporates the magnitude and the phase of CSI of each subcarrier for fingerprinting, but the phase information cannot be calibrated. In fact, the calibrated phase information obtained with a linear transformation is successfully used for line-of-sight (LOS) identification with WiFi [12] and passive human movement detection [13]. These two interesting works motivate us to explore calibrated CSI phase information for indoor fingerprinting.

In this paper, we present PhaseFi, an indoor fingerprinting system based on calibrated phase information of CSI. In PhaseFi, the raw phase information is first extracted from the CSI values from the 30 subcarriers of each of the three antennas of the Intel WiFi Link 5300 NIC (90 in total), by accessing the modified device driver. Then, by implementing a linear transformation to remove the phase offset, we obtain the calibrated phase information, which is shown in our measurement study to be more accurate than the raw phases. We also prove an upper bound for the variance of the calibrated phase, which clearly indicates its stability feature.

In the offline stage, unlike traditional shallow learning methods, we design a deep network with three hidden layers to train the calibrated phase data, and use weights to represent fingerprints, which can fully exploit the characteristic of the calibrated phase data. We also develop a greedy learning algorithm to train the weights in a layer-by-layer manner to effectively reduce the computational complexity. With this training approach, a sub-network between two continuous layers forms a Restricted Boltzmann Machine (RBM), which is solved by a contrastive divergence with one step iteration (CD-1) algorithm for sub-optimal solutions. Once the fingerprint database is established, the online stage uses a Bayes method based on the radial basis function (RBF) for location estimation. We also conduct extensive experiments to validate the performance of the PhaseFi system under two representative

978-1-4799-5952-5/15/$31.00 ©2015 IEEE

indoor environments. We find that PhaseFi outperforms other three benchmark schemes that are based on CSI or RSS in both scenarios.

In summary, the main contributions in this paper include:

1) We propose to use CSI phase information for indoor fingerprinting. Specifically, we theoretically prove and experimentally validate the feasibility of utilizing the calibrated phase information in CSI for indoor localization. To the best of our knowledge, this is the first work to leverage the calibrated phase information for indoor fingerprinting.
2) We design a deep network with three hidden layers to train the calibrated phase data, and utilize weights to represent fingerprints. We also develop a greedy learning algorithm to effective reduce the computational overhead for training. Furthermore, we present a Bayes method based on RBF for probabilistic location estimation.
3) We implement the PhaseFi system with commodity WiFi device and demonstrate its performance in two representative indoor environments. Experimental results show that PhaseFi outperforms several existing RSSI and CSI based schemes at only slightly increased execution time. The real-time localization requirement for indoor localization is satisfied.

The remainder of this paper is organized as follows. The preliminaries and phase sanitization are presented in Section II. We present PhaseFi in Section III and our experimental study in Section IV. Section V concludes this paper.

II. Preliminaries and Phase Sanitization

A. Channel State Information

In modern digital wireless communication systems, Orthogonal Frequency Division Multiplexing (OFDM) technique is widely used (e.g., in WiFi standards such as IEEE 802.11a/g/n). With OFDM, the total spectrum is divided into multiple orthogonal subcarriers and data is transmitted over the subcarriers using the same modulation scheme to combat frequency selective fading in multipath propagation environments. By modifying the device driver of off-the-shelf Network Interface Cards (NICs), such as Intel's IWL 5300, we are able to obtain Channel State Information (CSI) as fine-grained physical layer (PHY) information, which presents the subcarrier-level channel measurements in OFDM communications. In addition, CSI describes the channel properties experienced by the packet. For example, a wireless signal in propagation may undergo considerable impairments due to the shadowing, multipath effect, and power distortion, which are reflected in the CSI.

The WiFi channel at the 2.4 GHz band can be considered as a narrowband flat fading channel for OFDM systems. The channel model is defined as $\vec{Y} = \text{CSI} \cdot \vec{X} + \vec{N}$, where $\vec{Y}$ and $\vec{X}$ denote the received and transmitted signal vectors, respectively, $\vec{N}$ is the additive white Gaussian noise, and CSI represents the channel's frequency response, which can be obtained from $\vec{Y}$ and $\vec{X}$.

Although an 802.11a/g/n receiver implements an OFDM system with 56 subcarriers, the Intel WiFi Link 5300 NIC exports 30 out of 56 subcarriers via the device driver for each of its three antennas. The channel frequency response CSI_i of subcarrier i is a complex value, as follows $\text{CSI}_i = |\text{CSI}_i| \exp\{j\angle \text{CSI}_i\}$. In this paper, the proposed PhaseFi framework is based on the phases of the 30 subcarriers in the OFDM system, as discussed in the following.

B. Phase Sanitization

Although the phase of CSI is available from the Intel WiFi Link 5300 NIC, they have not been used for indoor localization yet. In fact, the problem is due to the random noise and unsynchronized timing between the transmitter and receiver, which lead to random phases and make raw phase information useless for localization. In this paper, we propose a simple yet effective approach to mitigate the random phase offsets by implementing a linear transformation.

Let $\angle\widehat{CSI}_i$ denote the measured phase of subcarrier i. It can be written as

$$\angle\widehat{CSI}_i = \angle \text{CSI}_i + 2\pi \frac{m_i}{N} \Delta t + \beta + Z, \tag{1}$$

where $\angle \text{CSI}_i$ is the genuine phase, Z is the measurement noise, Δt is the time lag, β is the unknown phase offset, m_i is the subcarrier index of the ith subcarrier, and N is the FFT size. We can obtain the subcarrier indices m_i for $i = 1$ to 30, and the FFT size N from the IEEE 802.11n specification [8]. In fact, because of the unknown Δt and β, it is impossible to obtain the genuine phase information. However, considering the phase across the total frequency band, we can implement a linear transformation on the raw phases to remove the terms of Δt and β [13].

Let k and b denote the slope of phase and the offset across the entire frequency band, respectively. We have

$$k = \frac{\angle\widehat{CSI}_{30} - \angle\widehat{CSI}_1}{m_{30} - m_1}, \quad b = \frac{1}{30}\sum_{i=1}^{30} \angle\widehat{CSI}_i. \tag{2}$$

Subtracting $km_i + b$ from the raw phase $\angle\widehat{CSI}_i$, we can obtain the calibrated phase $\angle\widetilde{CSI}_i$, which is given by

$$\angle\widetilde{CSI}_i = \angle\widehat{CSI}_i - km_i - b. \tag{3}$$

Theorem 1. *When the indices of 30 subcarriers are symmetric (i.e., ranging from -28 to 28 as in IEEE 802.11n) and the true phases of the 30 subcarriers are i.i.d., an upper bound of the variance of the calibrated phase is given by*

$$\text{Var}(\angle\widetilde{CSI}_i) \leq \frac{23}{15}\text{Var}(\angle CSI_i). \tag{4}$$

Proof: According to (1), we can compute the slope of the phase $k = \frac{\angle CSI_{30} - \angle CSI_1}{m_{30} - m_1} + \frac{2\pi}{N}\Delta t$, and the offset across the total frequency band $b = \frac{1}{30}\sum_{i=1}^{30} \angle CSI_i + \frac{2\pi\Delta t}{30N}\sum_{i=1}^{30} m_i + \beta + Z$. Since the indices of the 30 subcarriers are symmetric for IEEE 802.11n [13], we have $\sum_{i=1}^{30} m_i = 0$. It follows that $b = \frac{1}{30}\sum_{i=1}^{30} \angle CSI_i + \beta + Z$. Substituting the slope of the

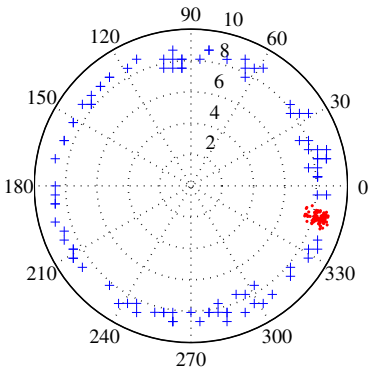

Fig. 1. Raw phase and calibrated phase measurements.

phase, k, the offset, b, and the measured phase of subcarrier i, $\angle\widetilde{CSI}_i$, into (3), the calibrated phase is given by

$$\angle\widetilde{CSI}_i = \angle CSI_i - \frac{\angle CSI_{30} - \angle CSI_1}{m_{30} - m_1} m_i - \frac{1}{30}\sum_{i=1}^{30} \angle CSI_i.$$

Note that the calibrated phase is a linear combination of the true phases, with the random offset β and time lag Δt removed. Since the true phases of the 30 subcarriers are i.i.d., the variance of the calibrated phase is $\text{Var}(\angle\widetilde{CSI}_i) = \text{Var}(\angle CSI_i) + \frac{m_i^2}{(m_{30}-m_1)^2}(\text{Var}(\angle CSI_{30}) + \text{Var}(\angle CSI_1)) + \text{Var}(\frac{1}{30}\sum_{i=1}^{30}\angle CSI_i)$. Since the subcarrier indices are symmetric, we have $m_i \leq m_{30}$ and $m_{30} = -m_1$, and it follows that $\frac{m_i^2}{(m_{30}-m_1)^2} \leq \frac{m_{30}^2}{(2m_{30})^2} = \frac{1}{4}$. Furthermore, since the true phases of the 30 subcarriers are i.i.d., we have $\text{Var}(\frac{1}{30}\sum_{i=1}^{30}\angle CSI_i) = \frac{1}{30}\text{Var}(\angle CSI_i)$ and $\text{Var}(\angle CSI_i) = \text{Var}(\angle CSI_{30}) = \text{Var}(\angle CSI_1)$. We thus have $\text{Var}(\angle\widetilde{CSI}_i) \leq \frac{23}{15}\text{Var}(\angle CSI_i)$, which completes the proof. ■

Theorem 1 provides an upper bound on the variance of the calibrated phase, and indicates that the calibrated phase is relatively stable. In Fig. 1, we plot the raw phases (as blue crosses) and the calibrated phases (as red dots) in the polar coordinate system for 100 CSI data units for the 8th subcarrier in the first antenna of the Intel WiFi link 5300 NIC. It can be easily seen that the raw phases scatter randomly over all feasible angles. This is why it is not useful for indoor localization. However, the calibrate phases, after the proposed linear transformation, all concentrate into a sector between 330° and 0°. The proposed linear transform does remove the phase offset, and the calibrate phases would be useful for indoor fingerprinting.

III. The PhaseFi System

A. System Architecture

The system architecture of PhaseFi is shown in Fig. 2. In our design, PhaseFi requires one mobile device equipped with an Intel WiFi link 5300 NIC, which can read CSI data from the slight modified device driver. The Intel WiFi link 5300 NIC has three antennas, each of which receives from 30 subcarriers. Thus we can collect 90 CSI data units for

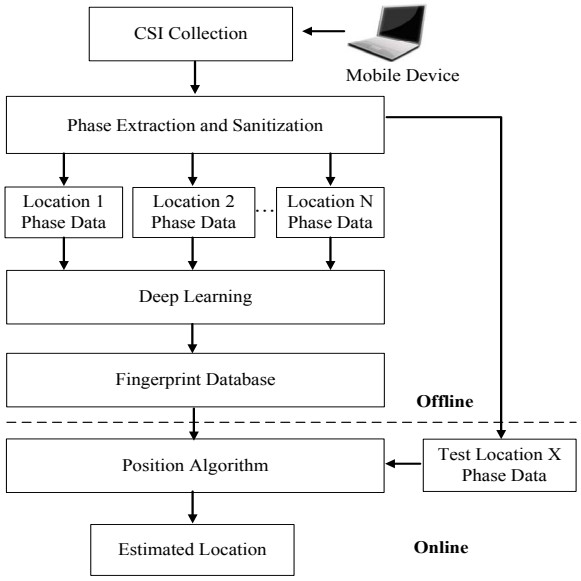

Fig. 2. Architecture of the proposed PhaseFi system.

one packet reception. Since all the subcarriers are considered, PhaseFi can effectively improve the diversity of training samples in deep learning, and is thus effective in exploiting the location features for building the fingerprint database. Then, the calibrated phases are obtained by implementing the proposed linear transformation on the the raw phases extracted from CSI data. PhaseFi considers the phase data for indoor fingerprinting for two reasons. First, when a signal encounters obstacle blockages, the amplitude of the signal will be strongly weakened, but the phase of the signal with the periodical change over the propagation distance is relatively more robust. Second, the calibrated phase information is relatively stable for a given position.

Once the calibrated phases are obtained, we use them for offline training and online test. In the offline training stage, PhaseFi incorporates deep learning to generate feature-based fingerprints. This approach is different from the traditional methods that directly store the measurement data as fingerprints, which are easily influenced by the complex indoor propagation environment. In addition, a large number of weights in the deep network are used as features-based fingerprints, which effectively represent the characteristics of the calibrated phases for each position. We create the fingerprint database by training the weights of the deep networks with calibrated phases for different positions. In the online test stage, a probabilistic data fusion approach is used to estimate the mobile device location based on the fingerprint database and the new calibrated phase data.

B. Offline Training

In the offline training stage, PhaseFi incorporates deep learning to train weights and then stores them to build feature-based fingerprint database. The training procedure consists of three stages: pretraining, unrolling, and fine-tuning [14]. In the pretraining stage, we use a deep network with one input

layer (with K_0 inputs) and three hidden layers (each with K_i nodes, $k = 1, 2, 3$). Let h^i denote the hidden variable with the K_i nodes at layer i, $i = 1, 2, 3$, and h^0 denote the calibrated phase data. In addition, we denote W_1, W_2 and W_3 as the weights between the calibrated phase data and the first hidden layer, the first and second hidden layer, and the second and third hidden layer, respectively.

Let $\Pr(h^0, h^1, h^2, h^3)$ denote the probabilistic generative model for the deep network with one input layer and three hidden layers. To obtain the optimal weights in the pretraining stage, we need to maximize the marginal distribution of the calibrated phase data for the deep network, which is formulated by

$$\max_{\{W_1,W_2,W_3\}} \sum_{h^1} \sum_{h^2} \sum_{h^3} \Pr(h^0, h^1, h^2, h^3). \tag{5}$$

Due to the complex model structure with multiple hidden layers and a large number of nodes in the deep network, it is challenging to obtain the optimal weights using the calibrated phase data with the maximum likelihood method. In PhaseFi, we develop a greedy learning algorithm to train the weights layer-by-layer by using a stack of RBMs to reduce complexity [15]. For the layer i RBM model, $i = 1, 2, 3$, the joint distribution $\Pr(h^{i-1}, h^i)$ is expressed by an RBM as a bipartite undirected graphical model [15], which is given by

$$\Pr(h^{i-1}, h^i) = \frac{\exp(-\mathbb{E}(h^{i-1}, h^i))}{\sum_{h^{i-1}} \sum_{h^i} \exp(-\mathbb{E}(h^{i-1}, h^i))}, \tag{6}$$

where $\mathbb{E}(h^{i-1}, h^i)$ represents the free energy between layer $i-1$ and layer i. $\mathbb{E}(h^{i-1}, h^i)$ is defined as

$$\mathbb{E}(h^{i-1}, h^i) = -b^{i-1}h^{i-1} - b^i h^i - h^{i-1} W_i h^i, \tag{7}$$

where b^{i-1} and b^i are the biases for units of layer $i-1$ and units of layer i, respectively. In fact, since it is difficult to find the joint distribution $\Pr(h^{i-1}, h^i)$, we use the CD-1 algorithm to approximate it as follows.

$$\begin{cases} \Pr(h^{i-1}|h^i) = \prod_{j=1}^{K_{i-1}} \Pr(h_j^{i-1}|h^i) \\ \Pr(h^i|h^{i-1}) = \prod_{j=1}^{K_i} \Pr(h_j^i|h^{i-1}), \end{cases} \tag{8}$$

where $\Pr(h_j^{i-1}|h^i)$, and $\Pr(h_j^i|h^{i-1})$ are described by sigmoid belief network, that are

$$\begin{cases} \Pr(h_j^{i-1}|h^i) = \left[1 + \exp\left(-b_j^{i-1} - \sum_{t=1}^{K_i} W_i^{j,t} h_t^i\right)\right]^{-1} \\ \Pr(h_j^i|h^{i-1}) = \left[1 + \exp\left(-b_j^i - \sum_{t=1}^{K_{i-1}} W_i^{j,t} h_t^{i-1}\right)\right]^{-1}. \end{cases} \tag{9}$$

We use the greedy algorithm to estimate the parameters of all weights for a stack of RBMs. First, given the calibrated phase data, the parameters $\{b^0, b^1, W_1\}$ of the first layer RBM are estimated by using CD-1 method. Then we freeze the parameters $\{b^0, W_1\}$ of the first layer, and sample from the conditional probability $\Pr(h^1|h^0)$ to train the parameters $\{b^1, b^2, W_2\}$ of the second layer RBM. Next, the parameters $\{b^0, b^1, W_1, W_2\}$ of the first and second layers are frozen, and then we sample from the conditional probability $\Pr(h^2|h^1)$ to train the parameters $\{b^2, b^3, W_3\}$ of the third layer RBM.

To update the weights in each RBM, the CD-1 method is adopted to approximate them. For the layer i RBM model, First, $\hat{h}^{i-1}$ is estimated by sampling from the conditional probability $\Pr(h^{i-1}|h^i)$. Then $\hat{h}^i$ is obtained by sampling from the conditional probability $\Pr(h^i|\hat{h}^{i-1})$. Finally, the parameters are updated as follows.

$$\begin{cases} \Delta W_i = \epsilon(h^{i-1}h^i - \hat{h}^{i-1}\hat{h}^i) \\ \Delta b^i = \epsilon(h^i - \hat{h}^i) \\ \Delta b^{i-1} = \epsilon(h^{i-1} - \hat{h}^{i-1}), \end{cases} \tag{10}$$

where ϵ is the step size.

Once the pretraining stage is completed, we obtain the near-optimal weights for the deep network. Then, in the unrolling stage, the reconstructed calibrated phase data are obtained by unrolling the deep network with forward propagation. Finally, we use the back-propagation algorithm to train all weights in the deep network by computing the error between the input calibrated phase data and the reconstructed calibrated phase data. This stage is called fine-tuning. After minimizing the error, the optimal weights are stored in the fingerprint database.

C. Position Algorithm

In the online test stage, a probabilistic method is developed to estimate the location of the mobile device based on the fingerprint database and new calibrated phase data. We compute the posteriori probability $\Pr(l_i|h^0)$ based on Bayes' law, which is given by $\Pr(l_i|h^0) = \frac{\Pr(l_i)\Pr(h^0|l_i)}{\sum_{i=1}^{N}\Pr(l_i)\Pr(h^0|l_i)}$, where N is the number of reference locations, l_i is reference location i in the fingerprint database, $\Pr(l_i)$ is the prior probability that the mobile device is determined to locate at the reference location l_i. We assume that $\Pr(l_i)$ follows an uniformly distribution, and then the posteriori probability $\Pr(l_i|h^0)$ can be simplified as follows. $\Pr(l_i|h^0) = \frac{\Pr(h^0|l_i)}{\sum_{i=1}^{N}\Pr(h^0|l_i)}$. Based on the deep network model, we consider $\Pr(h^0|l_i)$ as the RBF in the form of a Gaussian function to measure the degree of similarity between the reconstructed calibrated phase data $\hat{h^0}$ and the input calibrated phase data h^0, which is given by

$$\Pr(h^0|l_i) = \exp\left(-\frac{1}{\lambda\sigma}\left\|h^0 - \hat{h^0}\right\|\right), \tag{11}$$

where σ is the variance and λ is the parameter of the variance of the input calibrated phase data. Finally, the position of the mobile device can be computed as a weighted average of all the reference locations, as

$$\hat{l} = \sum_{i=1}^{N} \Pr(l_i|h^0) l_i. \tag{12}$$

IV. Experimental Validation

A. Experiment Methodology

We examine the performance of PhaseFi with extensive experiments. In our experiments, a TP Link router serves as AP and the mobile device is a Dell laptop equipped with an Intel WiFi Link 5300 NIC. At the mobile device, we design a Java program to continuously Ping the AP at a rate of 20

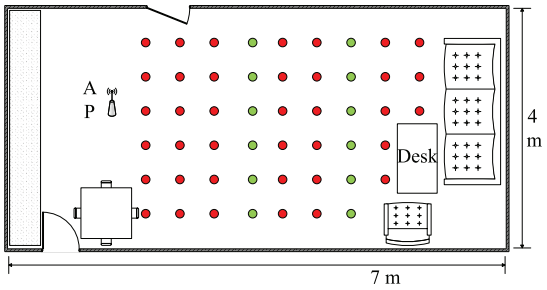

Fig. 3. Layout of the living room for training/test positions.

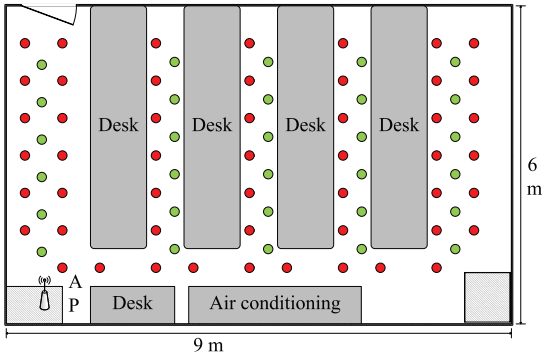

Fig. 4. Layout of the laboratory for training/test positions.

Pings per second. We also modify the NIC's device driver to read CSI values that are recorded in the hardware in the form of CSI for each packet reception. Then the phase data are extracted from the CSI and calibrated for training and testing. In this section, we validate the performance of PhaseFi in two representative indoor environments as follows.

1) Living Room: First, we perform experiments in a 4×7 m^2 living room where there are no outstanding obstacles around the center so that most of the measured locations can have LOS receptions. Fig. 3 shows the layout of the living room as well as the training/test points. The AP is placed at one end (rather than the center) of the living room on the floor to avoid isotropy. We set 38 points as training points (in red) and 12 points as test points (in green). In addition, we collect CSI data for 400 packet receptions for each training point, and 20 packet receptions for each test point. A deep network with structure $K_0 = 90$, $K_1 = 60$, $K_2 = 30$, and $K_3 = 15$ is used for the living room environment.

2) Computer Laboratory: Second, we chose a computer laboratory in Broun Hall in the campus of Auburn University. In this 6×9 m^2 laboratory, there are PCs and many desks crowded in the room such that most of the LOS paths are blocked, thus leading to a complex radio propagation environment. Fig. 4 shows the layout of the laboratory, where we select 50 training points and 30 test points. To obtain integrated characteristics of the subcarriers, we read CSI data for 800 packet receptions for each training point, and 20 packet receptions for each test point. The structure of the deep network in the laboratory environment is the same as that in the living room environment.

TABLE I
MEAN ERRORS AND EXECUTION TIME (LIVING ROOM)

Algorithm	*Mean error (m)*	*Std. dev. (m)*	*Mean exe. time (s)*
PhaseFi	1.0800	0.4046	0.3780
FIFS	1.2436	0.5705	0.2362
Horus	1.5449	0.7024	0.2297
ML	2.1615	1.0416	0.2290

TABLE II
MEAN ERRORS AND EXECUTION TIME (LABORATORY)

Algorithm	*Mean error (m)*	*Std. dev. (m)*	*Mean exe. time (s)*
PhaseFi	2.0134	1.0139	0.3770
FIFS	2.3304	1.0219	0.2439
Horus	2.5996	1.4573	0.2214
ML	2.8478	1.5545	0.2220

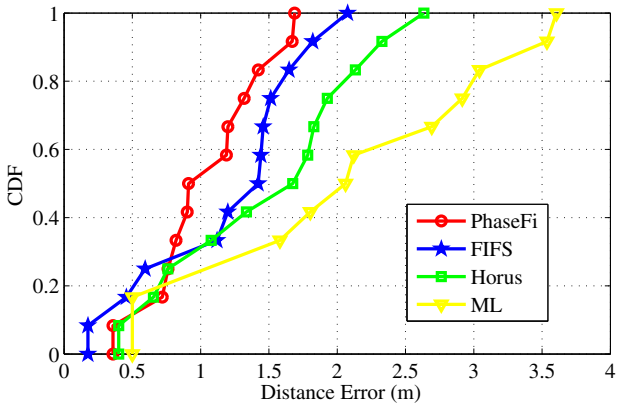

Fig. 5. CDF of localization errors of the living room experiments.

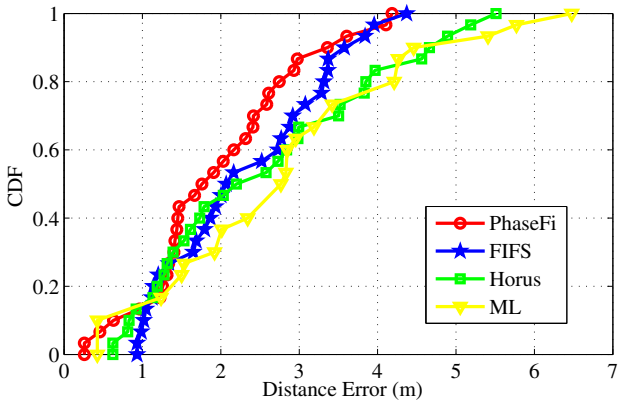

Fig. 6. CDF of localization errors of the laboratory experiments.

3) Benchmarks: For comparison purpose, we implement three existing methods, including FIFS [9], Horus [6], and Maximum Likelihood (ML) [16]. FIFS and Horus are introduced in Section I. In ML, based on RSS measurements, only one reference location with maximum posterior probability is considered as the estimated result. For a fair comparison, all schemes use the same measured data set to estimate the position of the mobile device.

B. Localization Performance

Tables I and II present the mean location errors, the standard deviations, and the average execution times of the living room and the laboratory experiments, respectively. In the living room environment, we find PhaseFi to achieve a mean location error of 1.08 m and a standard deviation of 0.4046 m for the 12 test points. In the laboratory scenario, the error is higher due to abundant multipath and shadowing effect. Our system achieves a mean error of 2.0134 m and a standard deviation of 1.0139 m for the 30 test points. For indoor localization accuracy, PhaseFi based on calibrated phases outperforms all the other schemes (i.e., FIFS, Horus and ML) that are based on amplitudes. PhaseFi also demonstrates robust performance for different locations with the smallest standard deviation. We also examine the computational complexity of the schemes. Although the mean execution time for PhaseFi is higher than the benchmark schemes, the 0.38 s average execution time of PhaseFi for both scenarios still satisfies the real-time requirement for most indoor localization applications. In fact, by optimizing the parameters and reducing the number of nodes in the deep network, the average execution time of PhaseFi can be further reduced.

Fig. 5 shows the cumulative distribution functions (CDF) of distance errors with the four schemes in the living room scenario. For PhaseFi, more than 50% of the test points have an error under 0.9 m using one AP, while the other schemes guarantee that 30% of the test points have an error under 0.9 m. Moreover, PhaseFi and FIFS have approximate 80% of the test points with mean location errors under 1.5 m, while Horus and ML have the same test points with mean error under 2.0 m and 3.0 m, respectively. The CSI-based schemes such as PhaseFi and FIFS can utilize the fined-grained subcarrier information, and are thus more stable than the RSS-based schemes.

Fig. 6 presents the CDFs of distance errors achieved with the four schemes in the laboratory environment. In this more complex propagation environment, for PhaseFi, about 60% of the test points have a distance error under 2 m, while the other schemes have the same portion of test points with error under 2.7 m. We find PhaseFi to be the most accurate among the four schemes, because the phase of the signal periodically changes over the propagation distance, which is more robust than amplitude, especially in cluttered propagation environments. The signal amplitude is usually more vulnerable to transmission impairments, and the correlation between signal strength and propagation distance is usually weak in indoor scenarios. Thus PhaseFi outperforms the three amplitude based schemes (based on either CSI or RSS).

V. Conclusion

In this paper, we proposed PhaseFi, a phase fingerprinting system for indoor localization. In the system, the phase information is first extracted and calibrated from the three antennas of the Intel WiFi Link 5300 NIC by accessing the modified device driver. In the offline stage, we designed a deep network with three hidden layers to train the calibrated phase data, and used weights to represent fingerprints. To reduce complexity, a greedy learning algorithm was incorporated to train the weights layer-by-layer, where a sub-network between continuous two layers formed an RBM approximately solved by a CD-1 algorithm. In the online stage, a Bayes method based on RBF was used for location estimation. The proposed PhaseFi scheme was validated in two different indoor environments, and was shown to outperform three benchmark schemes based on either CSI or RSS in both scenarios.

Acknowledgment

This work is supported in part by the US National Science Foundation (NSF) under grant CNS-1247955 and the Wireless Engineering Research and Education Center (WEREC) at Auburn University.

References

[1] X. Wang, S. Mao, S. Pandey, and P. Agrawal, "CA2T: Cooperative antenna arrays technique for pinpoint indoor localization," in *Proc. MobiSPC 2014*, Niagara Falls, Canada, Aug. 2014, pp. 392–399.

[2] X. Wang, H. Zhou, S. Mao, S. Pandey, P. Agrawal, and D. Bevly, "Mobility improves LMI-based cooperative indoor localization," in *Proc. IEEE WCNC 2015*, New Orlean, LA, Mar. 2015, pp. 2215–2220.

[3] P. Bahl and V. N. Padmanabhan, "Radar: An in-building RF-based user location and tracking system," in *Proc. IEEE INFOCOM'00*, Tel Aviv, Israel, Mar. 2000, pp. 775–784.

[4] H. Liu, H. Darabi, P. Banerjee, and L. Jing, "Survey of wireless indoor positioning techniques and systems," *IEEE Trans. Syst., Man, Cybern. C*, vol. 37, no. 6, pp. 1067–1080, Nov. 2007.

[5] S. Dayekh, "Cooperative localization in mines using fingerprinting and neural networks," in *Proc. IEEE WCNC'10*, Sydney, Australia, Apr. 2010, pp. 1–6.

[6] M. Youssef and A. Agrawala, "The Horus WLAN location determination system," in *Proc. ACM MobiSys'05*, Seattle, WA, June 2005, pp. 205–218.

[7] K. Wu, J. Xiao, Y. Yi, D. Chen, X. Luo, and L. Ni, "CSI-based indoor localization," *IEEE Trans. Parallel Distrib. Syst.*, vol. 24, no. 7, pp. 1300–1309, July 2013.

[8] D. Halperin., W. J. Hu., A. Sheth., and D. Wetherall., "Predictable 802.11 packet delivery from wireless channel measurements," in *Proc. ACM SIGCOMM'10*, New Delhi, India, Sept. 2010, pp. 159–170.

[9] J. Xiao, K. Wu., Y. Yi, and L. Ni, "FIFS: Fine-grained indoor fingerprinting system," in *Proc. IEEE ICCCN'12*, Munich, Germany, July/Aug. 2012, pp. 1–7.

[10] X. Wang, L. Gao, S. Mao, and S. Pandey, "DeepFi: Deep learning for indoor fingerprinting using channel state information," in *Proc. IEEE WCNC 2015*, New Orlean, LA, Mar. 2015, pp. 1666–1671.

[11] Y. Chapre, A. Ignjatovic, A. Seneviratne, and S. Jha, "CSI-MIMO indoor WiFi fingerprinting system," in *Proc. IEEE LCN 2014*, Edmonton, Canada, Sep. 2014, pp. 202–209.

[12] C. Wu, Z. Yang, Z. Zhou, K. Qian, Y. Liu, and M. Liu, "PhaseU: Real-time LOS identification with WiFi," in *Proc. IEEE INFOCOM'15*, Hong Kong, China, Apr. 2015.

[13] K. Qian, C. Wu, Z. Yang, Y. Liu, and Z. Zhou, "PADS: Passive detection of moving targets with dynamic speed using PHY layer information," in *Proc. IEEE ICPADS'14*, Hsinchu, Taiwan, Dec. 2014, pp. 1–8.

[14] G. Hinton and R. Salakhutdinov, "Reducing the dimensionality of data with neural networks," *Science*, vol. 313, no. 5786, pp. 504–507, July 2006.

[15] Y. Bengio, P. Lamblin, D. Popovici, and H. Larochelle, "Greedy layer-wise training of deep networks," in *Advances in Neural Information Processing Systems 19 (Proc. NIPS'06)*, Vancouver, Canada, Dec. 2007, pp. 153–160.

[16] M. Brunato and R. Battiti, "Statistical learning theory for location fingerprinting in wireless LANs," *Elsevier Computer Netw.*, vol. 47, no. 6, pp. 825–845, Apr. 2005.